ECS Journal of Solid State
Science and Technology

The Electrochemical Society
Advancing solid state & electrochemical science & technology

ACCEPTED MANUSCRIPT • OPEN ACCESS

A Metal-Oxide Contact to -Ga2O3 Epitaxial Films and Relevant Conduction Mechanism

To cite this article before publication: Alessio Bosio *et al* 2020 *ECS J. Solid State Sci. Technol.* in press https://doi.org/10.1149/2162-8777/ab8f37

Manuscript version: Accepted Manuscript

Accepted Manuscript is "the version of the article accepted for publication including all changes made as a result of the peer review process, and which may also include the addition to the article by IOP Publishing of a header, an article ID, a cover sheet and/or an 'Accepted Manuscript' watermark, but excluding any other editing, typesetting or other changes made by IOP Publishing and/or its licensors"

This Accepted Manuscript is **© 2020 The Author(s). Published by IOP Publishing Ltd.**.

As the Version of Record of this article is going to be/has been published on a gold open access basis under a CC 4.0 licence, this Accepted Manuscript is available for reuse under the applicable CC licence immediately.

Everyone is permitted to use all or part of the original content in this article, provided that they adhere to all the terms of the applicable licence referred to in the article – either https://creativecommons.org/licenses/by/4.0/ or https://creativecommons.org/licenses/by-nc-nd/4.0/

Although reasonable endeavours have been taken to obtain all necessary permissions from third parties to include their copyrighted content within this article, their full citation and copyright line may not be present in this Accepted Manuscript version. Before using any content from this article, please refer to the Version of Record on IOPscience once published for full citation and copyright details, as permissions may be required. All third party content is fully copyright protected and is not published on a gold open access basis under a CC licence, unless that is specifically stated in the figure caption in the Version of Record.

View the article online for updates and enhancements.

This content was downloaded from IP address 185.250.46.138 on 05/05/2020 at 14:18

A Metal-Oxide Contact to ε-Ga2O3 Epitaxial Films and Relevant Conduction Mechanism

Journal:	*ECS Journal of Solid State Science and Technology*
Manuscript ID	JSS-100192.R1
Manuscript Type:	Research Paper
Date Submitted by the Author:	04-Apr-2020

Complete List of Authors:	Bosio, Alessio; University of Parma, Mathematical, Physical and Computer Science Borelli, Carmine; University of Parma, Mathematical, Physical and Computer Science Parisini, Antonella; University of Parma, Mathematical, Physical and Computer Science Pavesi, Maura; University of Parma, Mathematical, Physical and Computer Science Vantaggio, Salvatore; University of Parma, Mathematical, Physical and Computer Science Fornari, Roberto; University of Parma, Mathematical, Physical and Computer Science

Keywords:	Ohmic contacts, ε-Ga2O3, wide bandgap semiconductors, electrical characterization, Sputtering, Thin film growth, MOCVD

SCHOLARONE™
Manuscripts

Accepted Manuscript

A Metal-Oxide Contact to ε - Ga_2O_3 Epitaxial Films and Relevant Conduction Mechanism

Alessio Bosio,[z] Carmine Borelli, Antonella Parisini, Maura Pavesi, Salvatore Vantaggio and Roberto Fornari

Department of Mathematical, Physical and Computer Sciences, University of Parma, 43124 Parma, Italy

[z]E-mail: alessio.bosio@unipr.it, alessio.bosio28@gmail.com

Abstract: In this work, the conduction mechanisms across novel contacts to epitaxial films of pure phase epsilon-Ga_2O_3 (ε-Ga_2O_3) were investigated. Different structures made by sputtered metal and oxide thin films were tested as electrical contacts. I-V characteristics show heterogeneous behaviors, revealing different conduction mechanisms according to the applied bias. The results are interesting as they offer a viable method to obtain ohmic contacts on ε-Ga_2O_3, which is less studied than other gallium oxide polymorphs but may find application in new electronic and optoelectronic devices. The newly developed ohmic contacts allow to fabricate simple test devices and assess the potential of this material.

This paper is part of the JSS Focus Issue on Gallium Oxide Based Materials and Devices II.

Introduction

Wide-bandgap semiconductors, such as silicon carbide (SiC), gallium nitride (GaN) and gallium oxide (Ga_2O_3) have recently raised great interest thanks to their extraordinary physical properties [1]. A large energy bandgap, a high critical electric field and a small intrinsic carrier concentration make these materials suitable for the realization of electronic devices, which operate at temperature, voltage and frequency significantly higher than those based on silicon. Among these semiconductors, Ga_2O_3 is considered very attractive for the realization of power electronics [2-6], short wavelength photonics [7-9], gas sensors [10, 11] and spintronics devices [12].
Metal/semiconductor junction is the fundamental part of any electronic device, and its physical properties have a strong impact on the overall electrical performance. Consequently, a fundamental understanding of how contacts work is one of the main steps to achieve a successful device.
The carrier transport mechanism across the junction makes metal contacts either rectifying (Schottky) or nonrectifying (Ohmic). Ohmic contacts have linear and symmetric current-voltage (I-V) characteristic, while in a Schottky contact a potential barrier, inducing an asymmetric I-V profile, occurs.
Essentially, ohmic contacts with low contact resistance are required to reduce the on-resistance (R_{on}) in electronic power devices [13, 14]. However, the realization of ohmic contacts on wide-bandgap semiconductors represents a real challenge.
Following the Schottky-Mott theory, a good ohmic contact with a *n*-type doped semiconductor is obtained only if the work function (Φ_m) of the metal, used as electrode, matches the electron affinity of the semiconductor (χ_s). If this condition is not satisfied, charge carriers have to overcome the ($q\Phi_m$ - χ_s) barrier height to be able to travel from semiconductor to metal. In order to avoid this situation, metals with low work function are commonly used [15-17,1].
The preparation of ohmic contacts on β-Ga_2O_3 is well established and different structures, involving metals or oxide-based semiconductors, were proposed. Many studies have been already and some of these [18-22] have shown that for the realization of ohmic contacts the intermixing layer formed between the metal and β-Ga_2O_3 is crucial, rather the barrier height. For this reason, the formation of an intermediate semiconductor layer is stimulated by pre-treatments of the β-Ga_2O_3 film surface with plasma exposure [6], reactive ion etching [5] and/or by post-contact deposition thermal annealing [3, 8, 23]. As an alternative to the formation of a thin small-gap semiconductor layer between the contact and the β-Ga_2O_3 layer, a heavily surface doping via ion implantation of β-Ga_2O_3 was attempted [6, 24]. When an elemental metal is used, an ohmic contact is normally obtained only when a post-deposition heat treatment at high temperature (800°C-1000°C) is made. This greatly

Accepted Manuscript
For Review Only

1
2
3
4
5
6
7
8
9
10
11
12
13
14
15
16
17
18
19
20
21
22
23
24
25
26
27
28
29
30
31
32
33
34
35
36
37
38
39
40
41
42
43
44
45
46
47
48
49
50
51
52
53
54
55
56
57
58
59
60

restricts the choice of possible metals, because some of them react at high temperature with the Ga_2O_3 surface. Metal atoms can diffuse into Ga_2O_3, steal oxygen and form a thin insulating oxide layer. This process at the same time makes available free Ga atoms at the metal-Ga_2O_3 interface. As a consequence, a low melting point intermetallic layer is formed, which compromises the contact adhesion to Ga_2O_3 surface [18] and impedes the obtainment of a good contact.

In the case of orthorhombic ε-Ga_2O_3 polymorph, the use of high annealing temperature is not allowed, since the ε-phase is thermodynamically metastable. In fact, ε-Ga_2O_3 initiates a phase transformation at temperatures higher than 700 °C [25].

On the other hand, ε-Ga_2O_3 is an interesting material with possible application in electronic and optoelectronic devices (i.e. solar-blind detectors), for this reason it is important to develop low-temperature processes for efficient electrical contacts on the ε-phase.

In this paper we present, for the first time, new results on the fabrication of ohmic contacts on nominally undoped ε-Ga_2O_3 grown by Metal Organic Chemical Vapour Deposition (MOCVD). Different stacked layers composed of metals and oxides were tested to achieve optimal metal-semiconductor-metal (MSM) devices adequate for UV-C detection. In particular, we explored the possibility to realize reliable contacts on resistive devices for UVC detector applications. For this purpose, it is mandatory to know if the contacts behave ohmic, independently from their mutual distance.

Experimental procedures

The nominally undoped ε-Ga_2O_3 thin films utilized in this work were epitaxially grown by MOCVD on 2-inch c-oriented sapphire substrates. Room temperature (RT) resistivity of the samples was in the range ($10^6 \div 10^8$) $\Omega \cdot$cm (Tab. 1). In order to prevent any surface effects, ε-Ga_2O_3 films were first etched in a solution of hydrofluoric and nitric acid (HF 50% + HNO_3 50%) for 1 min and then sequentially rinsed in acetone, isopropanol, deionized water and finally dried in dry nitrogen.

The one-face planar geometry, used for the fabrication of the electrical contacts, is showed in Figure 1. Contacts, with an area of (0.4 x 0.04) cm^2 spaced with nominal increasing distances of L_1 = 0.02 cm, L_2 = 0.04 cm, L_3 = 0.08 cm and L_4 = 0.16 cm between the contact strips, are realized by means of a stencil metallic mask. In particular, metal films were deposited by direct current (d.c.) pulsed magnetron sputtering starting with 3-inch metal target. Ar ions were produced by applying a d.c. power density of 1.8 W/cm^2 with a superimposed pulsed frequency of 100 kHz under an Ar pressure of 0.7 Pa. The resulted deposition rate was in the range of (0.3 ÷ 0.5) nm/s.

Oxide films were deposited by a 13.56 MHz radio-frequency (r.f.) magnetron sputtering applying a r.f. power density of 0,7 W/cm^2 over a 3-inch ceramic target under an Ar pressure of 0.3 Pa.

This sputtering system is equipped with a special tool for avoiding, as much as possible, the electron bombardment of the growing film. The ε-Ga_2O_3 film is covered by the incoming Sn and O atoms, which kinetic energy is carefully controlled by using low voltage drop (180 V) to keep the glow discharge on, corresponding to a very low deposition rate. The small energy provided by these atoms is just enough for increasing the surface temperature, allowing the diffusion of Sn atoms into the very first superficial layer of the Ga_2O_3 film, but it is not sufficient to cause lattice damage.

Different metallization schemes, such as Ti/Au, ZnO/Ti/Au, ITO/Pt, realized on nominally undoped ε-Ga_2O_3 films, did not exhibit linear I-V characteristics at any temperature.

In both Ti/Au and ZnO/Ti/Au structures, the formation of a very resistive thin layer of titanium oxide TiO_2 at the interface between Ga_2O_3 and the contact layer occurs [18], already during the sputtering deposition. Although Ti forms an ohmic contact with β-Ga_2O_3, it is not thermodynamically stable with ε-Ga_2O_3. In fact, the free energy of formation of TiO_2 is more negative than that of ε-Ga_2O_3 resulting in the formation of an insulating oxide layer at the ε-Ga_2O_3/Ti interface. Even if the deposition is carried out at substrate temperatures as low as 80 °C, the energy of the sputtered Ti atoms impinging the surface of the Ga_2O_3 film may be higher than 10 eV. The surface thermalization of these atoms locally increases the temperature, leading to the formation of TiO_2.

Considering the ITO/Pt system, it is known that Pt could form PtO_x inside the ITO matrix resulting effective in increasing the surface work function of the ITO film [26]. In this condition the band alignment of Pt-doped ITO with ε-Ga_2O_3 rises the contact barrier causing a higher system resistance. Moreover, due to a weak sticking with the ε-Ga_2O_3 surface, the sputtered ITO film shows some cracks, which makes the procedure irreproducible

Accepted Manuscript
For Review Only

1 2 3 4 5 6 7 8 9 10 11 12 13 14 15 16 17 18 19 20 21 22 23 24 25 26 27 28 29 30 31 32 33 34 35 36 37 38 39 40 41 42 43 44 45 46 47 48 49 50 51 52 53 54 55 56 57 58 59 60

and not usable. In order to avoid this problem, a sticking layer, consisting of a 100 nm thick SnO_x film, is deposited by reactive sputtering on top of the ε-Ga_2O_3 layer prior to deposition of the ITO film [27].

Results and discussion

In view of the considerations made in the Experimental section, the following discussion will be focused on the system SnO_x-ITO. The two layers, with a thickness of 100 nm and 1000 nm respectively, were sequentially deposited by sputtering on top of ε-Ga_2O_3 thin films.
Voltage-sweep cycles (± 50V) and (± 200V) were applied to pairs of adjacent contacts and I-V characteristics were recorded at RT.
The first analysis, concerning 2-3, 3-4 and 4-5 pairs, exhibits a good ohmic behavior as it is shown in Figure 2a. Nevertheless, the slopes of the curves, which give the conductance among the contacts under investigation, do not reflect the geometric distance between adjacent contacts.
If the measurement is performed in sequence, starting from 1-2 and then moving to 2-3, 3-4 and 4-5 pairs, space charge phenomena are observed. For example, the spatial charge effect on contact 2, triggered by the measurement on contact 1-2, also affects the 2-3 measurement, since contact 2 is common to both tests. This unwanted effect has been avoided by contacting three different specimens of the same ε-Ga_2O_3 layer (#422 Ud a,b,c) and then carrying out individual I-V measurement on just a pair for each specimen. The results are shown in Figure 2b.
This spatial charge effect is more evident when the I-V characteristics are measured for the first time on as-grown samples. Actually, when the I-V measurement starts, the space charge builds up progressively, and the stationary condition is reached only after a certain time. This is well evidenced by the hysteresis of the I-V characteristics under positive bias sweep (from 0V to 50V and from 50V to 0V), Figure 3 (black and red circles). Reversing the contact polarity, another trend is obtained (blue and green circles of Figure 3), not symmetric with respect to the first cycle. In these conditions, the I-V characteristic changes continuously with time, making the study of the contact behavior very difficult.
Let us consider only the black circles of the I-V characteristic in Figure 3, which correspond to the very first measurement performed on the 1-2 pair: two different trends are clearly visible: the first at low voltage, from 0V to 20V shows a linear behavior, while the second from 20V to 200V is compatible with a Schottky barrier-like behavior.
The linear part of the I-V characteristic, blown-up in Figure 4a, is confirmed by a slope of 1.09 of the I-V plot in a Log-Log scale. This behavior may be explained by some mechanisms occurring at the interface between contact bi-layer and gallium oxide film: the SnO_x contact releases some Sn atoms that diffuse into the Ga_2O_3 to provide *n*-type doping [27]. Tof-SIMS and RBS investigations (not reported here) show that sputtering deposition could promote the formation of a very thin intermixing layer, due to the interaction between Sn atoms and the surface of the Ga_2O_3 film.
As a consequence, a very thin barrier could form at the SnO_x/Ga_2O_3 interface due to the high concentration of donor atoms. In this situation, electrons, coming from SnO_x, may pass through the barrier thanks to a Fowler-Nordheim Tunneling or a Direct Tunneling mechanism. This hypothesis could explain the linear behavior of the first part of the I-V characteristic of the 1-2 pair. The second part of the I-V characteristic, reported as Log I vs. $V^{1/2}$ in Figure 4b, shows the linear trend typical of Schottky or thermionic emission, which means a conduction mechanism ruled by:

$$I \propto T^2 \cdot \exp\left(a\,\frac{\sqrt{V}}{k_B T} - q\,\frac{\Phi_B}{k_B T}\right) \qquad (1)$$

Where T = absolute temperature, V = applied voltage, Φ_B = barrier height, k_B = Boltzmann constant and a is a constant that is independent on V and T but depends on the dynamic permittivity of ε-Ga_2O_3 and on the thickness of the conduction layer.
Why does the conduction mechanism change from tunneling through to passing over the potential barrier?
The Sn-doped interface layer, interposed between SnO_x and undoped Ga_2O_3, as shown in Figure 5a, plays a fundamental role for understanding the transition from linear to exponential conduction regime. The electron current through Ga_2O_3 is limited by the high resistance of the material and at low bias, only the weak tunneling current may flow. Increasing the applied potential, the current cannot increase proportionally, since electrons, coming from the contact, tend to accumulate widening the barrier and preventing tunneling. In this condition, conduction occurs by overcoming the barrier, following a Schottky-thermionic emission.

Accepted Manuscript
For Review Only

1 2 3 4 5 6 7 8 9 10 11 12 13 14 15 16 17 18 19 20 21 22 23 24 25 26 27 28 29 30 31 32 33 34 35 36 37 38 39 40 41 42 43 44 45 46 47 48 49 50 51 52 53 54 55 56 57 58 59 60

Moreover, it was observed that the electron current between adjacent contacts reaches a stationary condition only few minutes after having applied a certain voltage. This depends on the transient time necessary for stabilizing the space charge at the contact region.

The stationary condition is indeed reached faster by initially biasing the contact pairs for 5 min with high voltage (contact curing). That is 200 V for 5 minutes prior to voltage sweeps in the range (0V ± 200V). Following this procedure, the I-V characteristic of the 1-2 pair shows the behavior shown in Figure 6. In the inset, the linear plot is explained by a Schottky-thermionic emission (Log I as a function of $V^{1/2}$), without tunneling (linear trend) typical of the I-V characteristics taken before the contacts curing at high voltage. In other words, submitting contacts to high voltage for few minutes, the space charge accumulated at one of the Sn-doped Ga_2O_3/undoped Ga_2O_3 interfaces reaches a stationary condition and the predominant conduction mechanism is well-described by a Schottky-thermionic emission over the entire voltage range.

A second question arises: why does this conduction mechanism take place just for the 1-2 pair, while the other contact couples exhibit a linear behavior independently from time and bias? Geometric distance between strips distinguishes different contact pair. As it is clearly seen in Figure 1, this distance doubles passing from a contact couple to the adjacent one, starting from 0.02 cm for the 1-2 pair, arriving up to 0.16 cm for the 4-5 pair. The greater the distance the more Ga_2O_3 material contributes to the resistance between contacts. This consideration suggests a physical model on the distribution of the voltage drop (see Figure 5b), which considers the resistances included between the contacts strips [28, 29].

When a voltage drop V is applied to a contact pair, we distinguish three main contributions. Denoting the voltage drop on the first contact (metal-semiconductor), on semiconductor, and on the second contact (semiconductor-metal) as V_{Ci}, V_s, V_{Cj}, respectively, the total voltage drop is: $V = V_{Ci} + V_S + V_{Cj}$, corresponding to a total resistance $R = R_{Ci} + R_S + R_{Cj}$.

In the case of 1-2 pair, the contact resistance R_{C1} and R_{C2} are greater than the material resistance R_S, accordingly, almost all the voltage falls on the contact barrier, symbolized by R_{C1} and R_{C2}. As a consequence, the contribution of the contacts is predominant. On the contrary, for other pairs the contribution of semiconductor resistance increases stepwise reaching soon the condition: $Rs \gg R_{C1}$ and R_{C2}. In this situation almost of the voltage drops on Rs and only a weak polarization falls on R_{C1} and R_{C2}. Low voltage means tunnelling through the contact barrier, corresponding to a linear behaviour in the I-V characteristic, and so is the contribution of Rs, purely ohmic. This explains the linearity of the I-V characteristics always observed for all contact pairs other than 1-2.

Several Ga_2O_3 samples were tested and different I-V characteristics were observed, which not always are well-fitted by Schottky barrier model. For all the samples, the I-V characteristics, related to the 1-2 pair, were performed in stationary conditions, i.e. after high potential had been applied for 5 min. As expected, the low-voltage linear behavior in experimental curves always disappeared, since the measurements were taken after high voltage curing. However, in some cases, the recorded I-V characteristic was consistent with space-charge limited current (SCLC) or Poole-Frenkel (P-F) emissions [30, 31].

SCLC mechanism is expected to occur in low mobility semiconductors, when injected charge density exceeds the intrinsic carrier density of the material. When the transport mechanism is described by the SCLC model, V and I are correlated by $I \propto V^m$ with $m \geq 2$. By plotting current and voltage values in Log-Log scale it is possible to determine the exponent m. For trap free (TF-SCLC) regime, $m = 2$ while for exponentially distributed trap (EDT-SCLC) regime $m > 2$.

For #483 Ud1 sample, experimental data (Figure 7a) gave $m = 2{,}04$ at RT, implying TF-SCLC regime.

P-F transport on the other hand is characterized by emission of trapped electrons into the conduction band, through thermal excitation enhanced by electric field. Conduction mechanism via the P-F model is described by:

$$I \propto V \cdot exp(\frac{\beta\sqrt{V}-\phi}{K_B T}) \qquad (2)$$

where k_B and T have the usual meaning, ϕ is the barrier height of the trap and β is a coefficient related to the dielectric constant of the material ε_r by:

$$\beta = \sqrt{\frac{q^3}{d\pi\varepsilon_0\varepsilon_r}} \qquad (3)$$

where ε_0 is the vacuum permittivity and d is the width of the depletion region. For #475 Ud1 sample, the P-F model actually provides a good fit to the experimental data (Figure 7b).

Accepted Manuscript For Peer Review Only

From Eq. (2) I-V curve should scale as Log (I/V) versus $V^{1/2}$. This plot yields a straight line with slope proportional to β. We can estimate the width of the depletion zone as $d \sim 40\ \mu m$, by considering $\varepsilon_r = 10$. All the obtained results and the correlated conduction models are summarized in Table 1.
It should be noted that, for all these electrical measurements no differences, attributable to conduction anisotropy were observed using contact patterns differently oriented on the surfaces of the Ga2O3 films. Anisotropy should not be expected anyway, as the epsilon structure, though orthorhombic at the microscopic scale, is indeed "hexagonal" at the scale typical of electronic transport.

Conclusion

Good ohmic contacts were achieved by deposition of SnO_x + ITO bilayers on undoped ε-Ga_2O_3 films grown by MOCVD on c-oriented sapphire. This is the first thorough investigation of this contact system applied to ε gallium oxide. Interestingly, the good ohmic behavior was obtained without making use of any high-temperature treatment, which is an indispensable requirement for fabrication of electronic devices based on the metastable ε-Ga_2O_3 polymorph. Experimental results show that the ohmic behavior is obtained when a low-voltage bias is applied. The ohmicity being attributed to tunneling through a very thin barrier at the interface between SnO_x and ε-Ga_2O_3 surface, formed in consequence of heavy Sn-diffusion from the deposited contact. At higher voltage bias a linear trend is achieved only if the two contacts are sufficiently distant, i.e. if the resistive contribution from Ga_2O_3 dominates over the contribution from contact strips.
If the interface barrier becomes too wide, the tunneling is not permitted and carriers overcoming the contact barrier provide the main contribution to the transport across the MSM structure. In this case three different models could explain the non-linearity trend of the I-V characteristics: two of these models are related to trap-free interface, i.e. the Schottky-thermionic and space charge limited current emissions; the third model bases on the Pool-Frenkel mechanism, that takes place when the depleted zone extends laterally over a larger part of the ε-Ga_2O_3 layer between the contacts.

Acknowledgements

The authors wish to thank Dr. Matteo Bosi of IMEM-CNR Institute for supply of the ε-Ga_2O_3 films utilized in this work.

References

[1] S. J. Pearton, J. Yang, P. H. Cary IV, F. Ren, J. Kim, M. J. Tadjer and M. A. Mastro, Appl Phys Rev, **5**, 1, (2018).
[2] K. Irmscher, Z. Galazka, M. Pietsch, R. Uecker and R. Fornari, J Appl Phys, **110**, 063720, (2011).
[3] K. Sasaki, A. Kuramata, T. Masui, E. G. Víllora, K. Shimamura and S. Yamakoshi, Appl Phys Express, **5**, 03 5502, (2012).
[4] S. Müller, H. von Wenckstern, F. Schmidt, D. Splith, F. L. Schein, H. Frenzel and M. Grundmann, Appl Phys Express, **8**, (2015).
[5] M. Higashiwaki, K. Sasaki, K. Goto, K. Nomura, Q. T. Thieu, R. Togashi, H. Murakami, Y. Kumagai, B. Monemar, A. Koukitu, A. Kuramata and S. Yamakoshi, in 73rd Annual Device Research Conference (DRC), 29, IEEE, Columbus, OH, (2015).
[6] M. H. Wong, K. Sasaki, A. Kuramata, S. Yamakoshi and M. Higashiwaki, IEEE Electr Device L, **37**, 212, (2016).
[7] T. Oshima, T. Okuno, N. Arai, N. Suzuki, S. Ohira and S. Fujita, Appl Phys Express, **1**, 1202, (2008).
[8] R. Suzuki, S. Nakagomi, Y. Kokubun, N. Arai and S. Ohira, Appl Phys Lett, **94**, 222102-1, (2009).
[9] R. Suzuki, S. Nakagomi and Y. Kokubun, Appl Phys Lett, **98**, 131114-1, (2011).
[10] M. Ogita, N. Saika, Y. Nakanishi and Y. Hatanaka, Appl Surf Sci, **142**, 188, (1999).
[11] S. Nakagomi, T. Sai and Y. Kokubun, in 14th International Meeting on Chemical Sensors - IMCS 2012, 750, Nürnberg, DE, (2012).
[12] A. A. Dakhel and W. E. Alnaser, "Microelectron Reliab, **52**, 1050, (2012).
[13] F. Roccaforte, F. La Via and V. Raineri, IJHSES, **15**, 781, (2005).
[14] B. J. Baliga, Semicond Sci Technol, **28**, 074011, (2013).
[15] J. S. Foresi and T. D. Moustakas, Appl Phys Lett, **62**, 2859, (1993).
[16] G. Greco, F. Iucolano and F. Roccaforte, App Surf Sci, **383**, 324, (2016).
[17] S. N. Mohammad, J Appl Phys, **95**, 7940, (2004).

Accepted Manuscript
For Review Only

1
2
3
4
5
6
7
8
9
10
11
12
13
14
15
16
17
18
19
20
21
22
23

[18] Y. Yao, R. F. Davis and L. M. Porter, J Electron Mater, **46**, 2053, (2017).
[19] T. Oshima, R. Wakabayashi, M. Hattori, A. Hashiguchi, N. Kawano, K. Sasaki, T. Masui, A. Kuramata, S. Yamakoshi, K. Yoshimatsu, A. Ohtomo, T. Oishi and M. Kasu, Jpn J Appl Phys, **55**, 1, (2016).
[20] S. Jang, S. Jung, K. Beers, J. Yang, F. Ren , A. Kuramata , S. J. Pearton and K. H. Baik , J Alloy Compd, **731**, 118, (2018).
[21] J. D. Guo, C. I. Lin, M. S. Feng, F. M. Pan, G. C. Chi and C. T. Lee, Appl Phys Lett, **68**, 235, (1996).
[22] P. H. Carey, J. Yang, F. Ren, D. C. Hays, S. J. Pearton, S. Jang, A. Kuramata and I. I. Kravchenko, AIP Adv, **7**, 1, (2017).
[23] T. Oshima, T. Okuno, N. Arai, N. Suzuki, H. Hino e S. Fujita, Jpn J Appl Phys, **48**, 01 1605, (2009).
[24] K. Sasaki, M. Higashiwaki, A. Kuramata, T. Masui and S. Yamakoshi, Appl Phys Express, **6**, 08 6502, (2013).
[25] R. Fornari, M. Pavesi, V. Montedoro, D. Klimm , F. Mezzadri , I. Cora , B. Pécz, F. Boschi, A. Parisini, A. Baraldi, C. Ferrari, E. Gombia and M. Bosi, Acta Mater, **140**, 411, (2017).
[26] C. M. Hsu, C. Y. Huang, H. E. Cheng and W. T. Wu, J Phys D Appl Phys, **42**, 105301, (2009).
[27] A. Parisini, A. Bosio, V. Montedoro, A. Gorreri, A. Lamperti, M. Bosi, G. Garulli, S. Vantaggio, R. Fornari, APL Mater, **7**, 031114, (2019).
[28] F. C. Chiu, Adv Mater Sci Eng, **2014**, 1, (2014).
[29] Z. Zhang, K. Yao, Y. Liu, C. Jin, X. Liang, Q. Chen e L. M. Peng, Adv Funct Mater, **17**, 2478, (2007).
[30] M. Choueib, A. Ayari, P. Vincent, S. Perisanu and S. Purcell, J Appl Phys, **109**, 073709, (2011).
[31] D. Joung, A. Cunder, L. Zhai and S. I. Khondaker, Appl Phys Lett, **97**, 093105, (2010).

24
25
26
27
28
29
30
31
32
33
34
35
36
37
38
39
40
41
42
43
44
45
46
47
48
49
50
51
52
53
54
55
56
57
58
59
60

Accepted Manuscript
For Review Only

1
2
3
4
5
6
7
8
9
10
11
12
13
14
15
16
17
18
19
20
21
22
23
24
25
26
27
28
29
30
31
32
33
34
35
36
37
38
39
40
41
42
43
44
45
46
47
48
49
50
51
52
53
54
55
56
57
58
59
60

Table caption

Table 1. Information related to investigated samples. Resistance is extrapolated from the slope of the I-V characteristics carried out on 4-5 pair, where the contribution of the material (ε-Ga_2O_3 film) between contacts dominates. Resistivity is estimated from resistance values by considering the geometrical dimensions; note that for 4-5 pair $R_S \gg R_{C4}$ and R_{C5}. (S-B = Schottky-Barrier, P-F = Pool-Frenkel, TF-SCLC = Trap Free Space Charge Limited Current).

Accepted Manuscript
For Review Only

1
2
3
4
5
6
7
8
9
10
11
12
13
14
15
16
17
18
19
20
21
22
23
24
25
26
27
28
29
30
31
32
33
34
35
36
37
38
39
40
41
42
43
44
45
46
47
48
49
50
51
52
53
54
55
56
57
58
59
60

Table 1

Sample	Thickness (nm)	Contact layers	RT Ga_2O_3 Resistance (4-5 pair) (Ω)	RT Ga_2O_3 Resistivity (Ω·cm)	Conduction model (1-2 pair)
#422 Ud1	290	SnO_x + ITO	4×10^{10}	10^7	S-B
#475 Ud1	670	SnO_x + ITO	5×10^9	10^6	P-F
#483 Ud1	930	SnO_x + ITO	4×10^{11}	10^8	TF-SCLC

Table 1. Information related to investigated samples. Resistance is extrapolated from the slope of the I-V characteristics carried out on 4-5 pair, where the contribution of the material (ε-Ga_2O_3 film) between contacts dominates. Resistivity is estimated from resistance values by considering the geometrical dimensions; note that for 4-5 pair $R_S >> R_{C4}$ and R_{C5}. (S-B = Schottky-Barrier, P-F = Pool-Frenkel, TF-SCLC = Trap Free Space Charge Limited Current).

Accepted Manuscript

For Review Only

1 2 3 4 5 6 7 8 9 10 11 12 13 14 15 16 17 18 19 20 21 22 23 24 25 26 27 28 29 30 31 32 33 34 35 36 37 38 39 40 41 42 43 44 45 46 47 48 49 50 51 52 53 54 55 56 57 58 59 60

Figure captions

Figure 1. Contact configuration used for I-V measurements. L_1 = 0.02 cm, L_2 = 0.04 cm, L_3 = 0.08 cm and L_4 = 0.16 cm are the nominal distances between the contact strips.

Figure 2. (**a**) sample #422 Ud1, RT I-V characteristics measured on the 2-3, 3-4 and 4-5 pairs in non-stationary conditions; the slopes of the straight lines do not correspond to distances between the contact pads. (**b**) RT I-V characteristics of three different pieces (a, b, c) of the same layer (#422 Ud). In "a" only the 2-3 pair is contacted, while in "b" e "c" are contacted only the 3-4 and 4-5 pairs respectively; here the slopes of the straight lines do scale with the distances between the contact pads.

Figure 3. sample #422 Ud1, RT I-V characteristic measured on 1-2 contact pair in non-stationary conditions.

Figure 4. (**a**) RT I-V curve reported in Log-Log scale relative to Figure 3 (black circles) for low-voltage sweeps from 0V to 20V, exhibiting a linear tunneling mechanism. (**b**) The second part of the same characteristic is reported in Log I vs $V^{1/2}$ scale for higher-voltage sweep (20V to 50V), showing a Schottky-like behavior.

Figure 5. (**a**) Schematic of the ITO-SnOx contact to ε-Ga_2O_3 with the barrier formation at the interface layer. (**b**) schematic model for dual terminal ε-Ga_2O_3 system with highlighted the voltage drop distribution as a consequence of the resistive divider.

Figure 6. sample #422 Ud1, RT I-V characteristic measured in stationary conditions, bias of 200V for 5 min applied to the 1-2 pair. The inset shows Schottky conduction in the range 10V - 200V. Current values under ±10V bias are below the detectability treshold of the amperometer.

Figure 7. RT I-V characteristic measured between the 1-2 contacts, after preliminary curing at 200V for 5 min (stationary condition) (**a**) sample #483 Ud 1, the inset is the fitting of the SCLC model in 10V - 200V range. (**b**) sample #475 Ud 1. The inset represents the fitting of Pool-Frenkel model with positive applied bias; I-V characteristic is not completely symmetric with positive or negative bias since the contact pads are not identical.

Accepted Manuscript
For Review Only

1 2 3 4 5 6 7 8 9 10 11 12 13 14 15 16 17 18 19 20 21 22 23 24 25 26 27 28 29 30 31 32 33 34 35 36 37 38 39 40 41 42 43 44 45 46 47 48 49 50 51 52 53 54 55 56 57 58 59 60

Figure 1

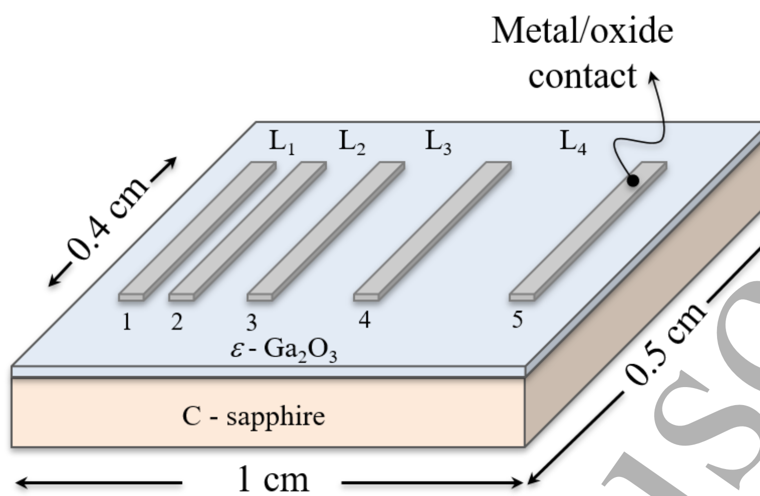

Figure 1. Contact configuration used for I-V measurements. L_1 = 0.02 cm, L_2 = 0.04 cm, L_3 = 0.08 cm and L_4 = 0.16 cm are the nominal distances between the contact strips.

Accepted Manuscript

Review Only

1
2
3
4
5
6
7
8
9
10
11
12
13
14
15
16
17
18
19
20
21
22
23
24
25
26
27
28
29
30
31
32
33
34
35
36
37
38
39
40
41
42
43
44
45
46
47
48
49
50
51
52
53
54
55
56
57
58
59
60

Figure 2

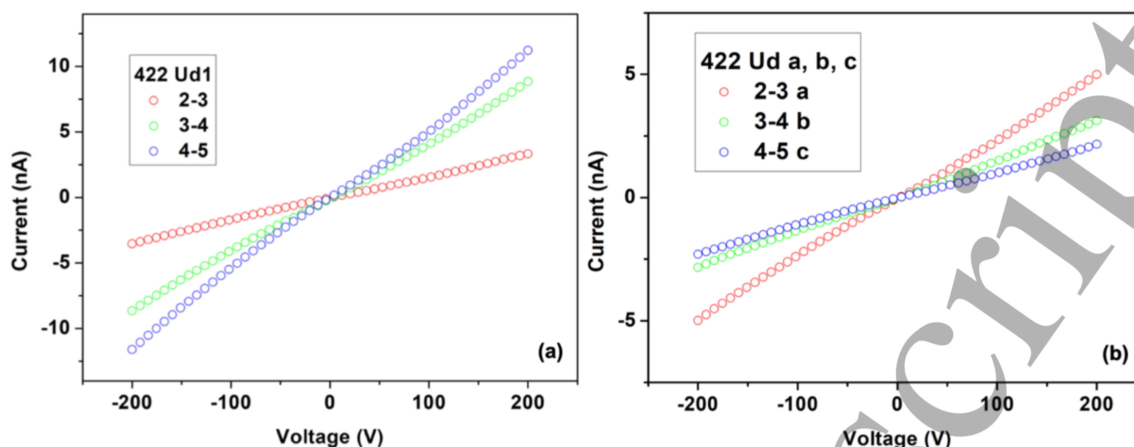

Figure 2. (**a**) sample #422 Ud1, RT I-V characteristics measured on the 2-3, 3-4 and 4-5 pairs in non-stationary conditions; the slopes of the straight lines do not correspond to distances between the contact pads. (**b**) RT I-V characteristics of three different pieces (a, b, c) of the same layer (#422 Ud). In "a" only the 2-3 pair is contacted, while in "b" e "c" are contacted only the 3-4 and 4-5 pairs respectively; here the slopes of the straight lines do scale with the distances between the contact pads.

Accepted Manuscript
For Review Only

1
2
3
4
5
6
7
8
9
10
11
12
13
14
15
16
17
18
19
20
21
22
23
24
25
26
27
28
29
30
31
32
33
34
35
36
37
38
39
40
41
42
43
44
45
46
47
48
49
50
51
52
53
54
55
56
57
58
59
60

Figure 3

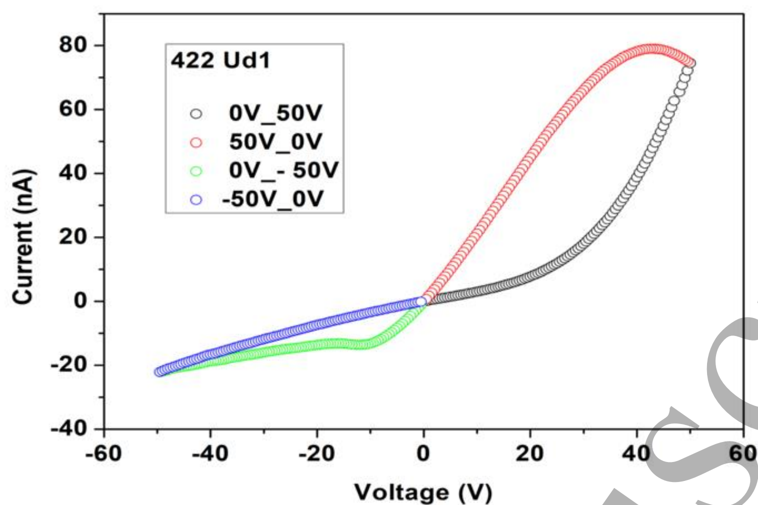

Figure 3. sample #422 Ud1, RT I-V characteristic measured on 1-2 contact pair in non-stationary conditions.

Accepted Manuscript
For Review Only

1
2
3
4
5
6
7
8
9
10
11
12
13
14
15
16
17
18
19
20
21
22
23
24
25
26
27
28
29
30
31
32
33
34
35
36
37
38
39
40
41
42
43
44
45
46
47
48
49
50
51
52
53
54
55
56
57
58
59
60

Figure 4

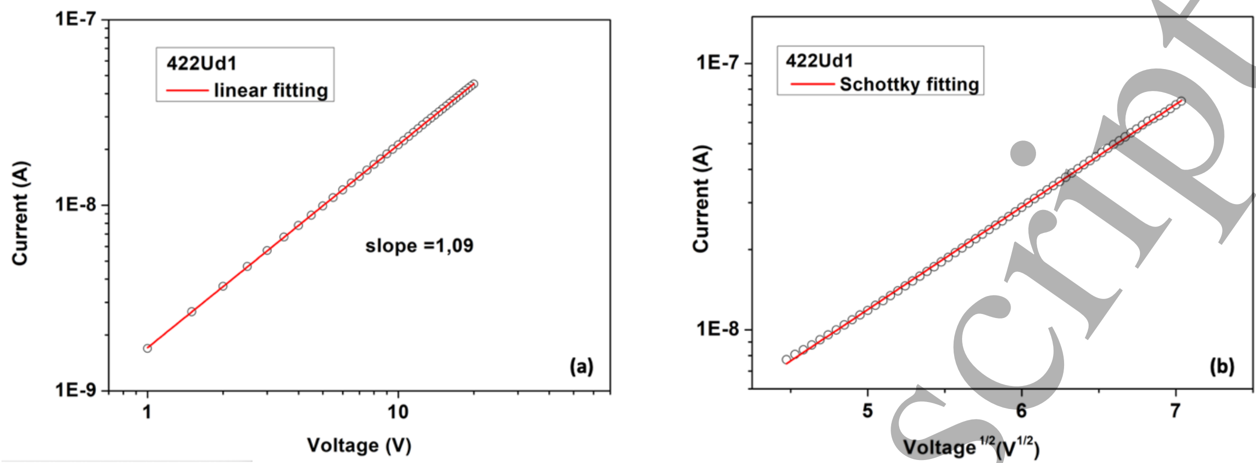

Figure 4. (**a**) RT I-V curve reported in Log-Log scale relative to Figure 3 (black circles) for low-voltage sweeps from 0V to 20V, exhibiting a linear tunneling mechanism. (**b**) The second part of the same characteristic is reported in Log I vs $V^{1/2}$ scale for higher-voltage sweep (20V to 50V), showing a Schottky-like behavior.

Accepted Manuscript
For Review Only

1
2
3
4
5
6
7
8
9
10
11
12
13
14
15
16
17
18
19
20
21
22
23
24
25
26
27
28
29
30
31
32
33
34
35
36
37
38
39
40
41
42
43
44
45
46
47
48
49
50
51
52
53
54
55
56
57
58
59
60

Figure 5

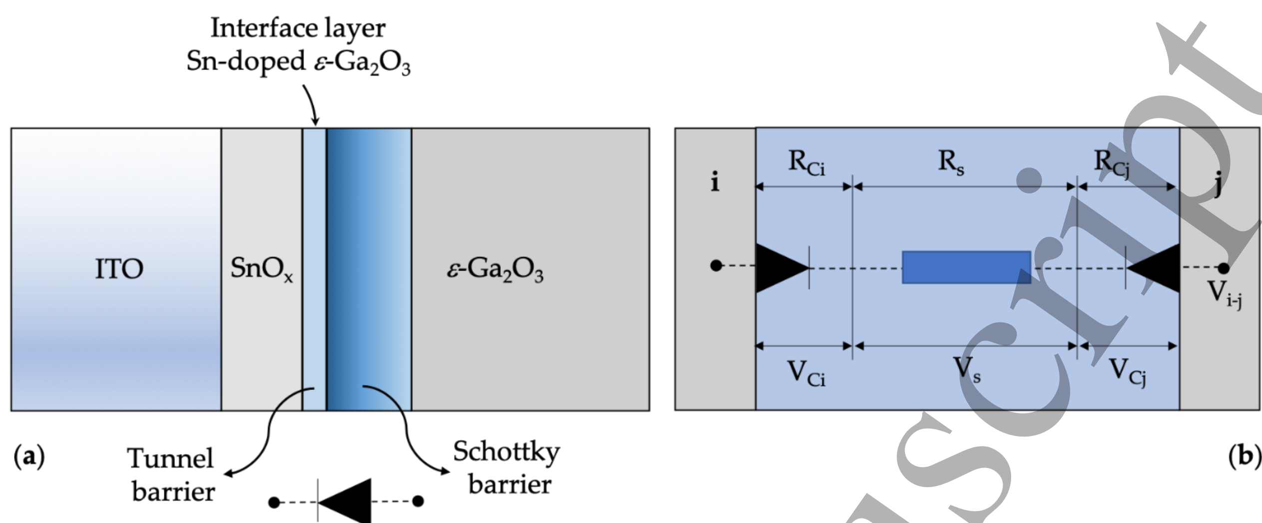

Figure 5. (**a**) Schematic of the ITO-SnOx contact to ε-Ga_2O_3 with the barrier formation at the interface layer. (**b**) schematic model for dual terminal ε-Ga_2O_3 system with highlighted the voltage drop distribution as a consequence of the resistive divider.

Accepted Manuscript
For Review Only

1
2
3
4
5
6
7
8
9
10
11
12
13
14
15
16
17
18
19
20
21
22
23
24
25
26
27
28
29
30
31
32
33
34
35
36
37
38
39
40
41
42
43
44
45
46
47
48
49
50
51
52
53
54
55
56
57
58
59
60

Figure 6

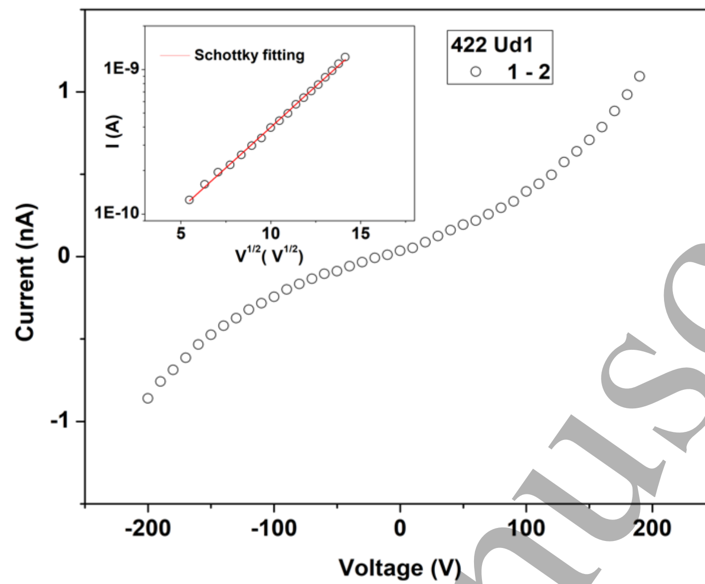

Figure 6. sample #422 Ud1, RT I-V characteristic measured in stationary conditions, bias of 200V for 5 min applied to the 1-2 pair. The inset shows Schottky conduction in the range 10V - 200V. Current values under ±10V bias are below the detectability treshold of the amperometer.

Accepted Manuscript
Review Only

1
2
3
4
5
6
7
8
9
10
11
12
13
14
15
16
17
18
19
20
21
22
23
24
25
26
27
28
29
30
31
32
33
34
35
36
37
38
39
40
41
42
43
44
45
46
47
48
49
50
51
52
53
54
55
56
57
58
59
60

Figure 7

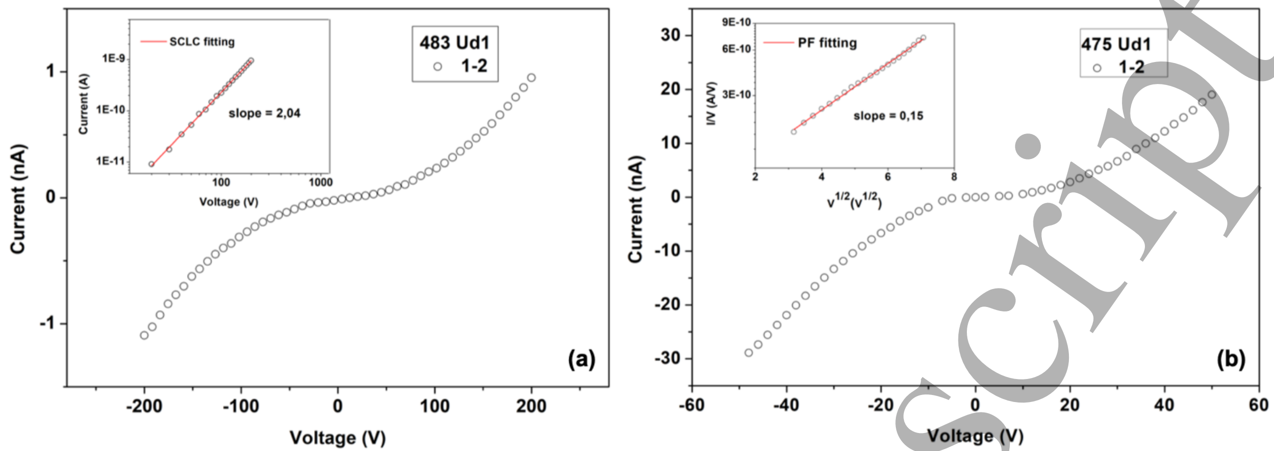

Figure 7. RT I-V characteristic measured between the 1-2 contacts, after preliminary curing at 200V for 5 min (stationary condition) (**a**) sample #483 Ud 1, the inset is the fitting of the SCLC model in 10V - 200V range. (**b**) sample #475 Ud 1. The inset represents the fitting of Pool-Frenkel model with positive applied bias; I-V characteristic is not completely symmetric with positive or negative bias since the contact pads are not identical.

Accepted Manuscript
For Review Only